


## Original Research Article

An engineered *Yarrowia lipolytica* with rapid growth and efficient lipid utilizationTianyu Dong<sup>a,c</sup>, Yujie Shu<sup>a,c</sup>, Ying Wang<sup>a,c</sup>, Mingdong Yao<sup>a,c,\*</sup>,  
Wenhai Xiao<sup>a,b,c,d,\*\*</sup> <sup>a</sup> Frontiers Science Center for Synthetic Biology and Key Laboratory of Systems Bioengineering (Ministry of Education), School of Chemical Engineering and Technology, Tianjin University, Tianjin, 300072, China<sup>b</sup> School of Life Science, Faculty of Medicine, Tianjin University, Tianjin, 300072, China<sup>c</sup> Frontier Research Institute for Synthetic Biology, Tianjin University, Tianjin, 300072, China<sup>d</sup> Georgia Tech Shenzhen Institute, Tianjin University, Shenzhen, 518071, China

## ARTICLE INFO

## Keywords:

*Yarrowia lipolytica*

Cell growth

Lipid accumulation

Acetyl-CoA accumulation

 $\beta$ -carotene

## ABSTRACT

*Yarrowia lipolytica*, a safe yeast, efficiently metabolizes lipids for the production of food additives and agricultural products. Boosting its growth and lipid utilization capabilities is crucial to enhancing the overall efficiency of *Y. lipolytica*. Herein, an integrated strategy was implemented to enhance lipid uptake, accumulation and metabolism and systematically promote the growth and lipid utilization of the commonly used *Y. lipolytica* Po1f strain. The engineered strain had a specific growth rate of  $0.32\text{ h}^{-1}$  and a lipid content of 67.66 % (g/g DCW), which were 54 % and 26 % greater than those of the original strain.  $\beta$ -Carotene was used to verify the production of lipophilic natural compounds, and the highest yield was obtained 48 h earlier using the engineered strain compared to the original strain when consuming same carbon source. These findings show promise in using engineered *Y. lipolytica* for rapid growth and improved lipid utilization to boost efficiency of lipophilic product production.

## 1. Introduction

*Yarrowia lipolytica*, an unconventional yet promising yeast species, has garnered great attention after it was granted generally recognized as safe (GRAS) status by the FDA. Its unique capabilities and ability to ensure its safety have positioned it as a versatile and reliable microbial platform for crafting food additives, pharmaceutical products, and cosmetic ingredients. Owing to its swift growth and exceptional ability to metabolize and assimilate hydrophobic substrates as the sole carbon source, it has emerged as a highly promising bioproduction platform that utilizes oils and fats [1,2]. Initially, renowned as a source of single-cell protein, *Y. lipolytica* can benefit the production of value-adding products. Recently, the production of squalene, a natural antioxidant, was greatly increased by improving the homologous recombination efficiency of *Y. lipolytica* [3]. Additionally, the efficient

biosynthesis of retinol, a notable antiaging drug, was achieved by the fed-batch fermentation of *Y. lipolytica* in a 5 L bioreactor, resulting in a noteworthy total retinol yield of 5.4 g/L [4].

With advancements in genetic engineering tools and fermentation strategies, *Y. lipolytica* has emerged as a top contender for various large-scale biomanufacturing processes [5,6]. However, the engineered version of *Y. lipolytica* often has a slower growth rate than its original strain does, particularly following the extensive rewiring of its metabolic pathway, significantly impeding its use in bioproduction processes [7]. Optimizing chassis cells not only facilitates the synthetic biology modification process but also underscores its advantages in yielding a diverse range of products. Consequently, the cultivation of fast-growing *Y. lipolytica* holds great potential for improving bioproduction processes. Previous studies revealed that the deletion or overexpression of genes in a multigene family in *Y. lipolytica*, *UP1–UP4*, reduces or enhances

Peer review under the responsibility of Editorial Board of Synthetic and Systems Biotechnology.

\* Corresponding author. Frontiers Science Center for Synthetic Biology and Key Laboratory of Systems Bioengineering (Ministry of Education), School of Chemical Engineering and Technology, Tianjin University, Tianjin, 300072, China.

\*\* Corresponding author. Frontiers Science Center for Synthetic Biology and Key Laboratory of Systems Bioengineering (Ministry of Education), School of Chemical Engineering and Technology, Tianjin University, Tianjin, 300072, China.

E-mail addresses: [mingdong.yao@tju.edu.cn](mailto:mingdong.yao@tju.edu.cn) (M. Yao), [wenhai.xiao@tju.edu.cn](mailto:wenhai.xiao@tju.edu.cn) (W. Xiao).<https://doi.org/10.1016/j.synbio.2025.01.007>

Received 8 October 2024; Received in revised form 29 December 2024; Accepted 20 January 2025

Available online 26 January 2025

2405-805X/© 2025 The Authors. Publishing services by Elsevier B.V. on behalf of KeAi Communications Co. Ltd. This is an open access article under the CC BY-NC-ND license (<http://creativecommons.org/licenses/by-nc-nd/4.0/>).

octanoic acid sensitivity, indicating their potential role in binding extracellular fatty acids [8]. Moreover, the overexpression of the multi-copy DGAT gene *DGA1* profoundly influences the dimensions of lipid bodies present within *Y. lipolytica* cells, leading to an increase in lipid accumulation [9]. The  $\beta$ -oxidation pathway, a fundamental metabolic route for the degradation of fatty acids, is intricately orchestrated by six peroxisomal acyl-CoA oxidases, each encoded by *POX1–6*. These enzymes display specific preferences for fatty acid chains of different lengths, ensuring a tailored approach to the breakdown process. Previous investigations revealed a crucial connection between the functionality of these *POX1–6*-encoded oxidases and the overall fatty acid degradation capacity of *Y. lipolytica* strains. Specifically, mutations within the *POX1–6* genes have been shown to compromise the ability of these strains to efficiently degrade fatty acids, resulting in a conspicuous accumulation of lipids within the biomass [10]. The subsequent stages of  $\beta$ -oxidation are facilitated by a multifunctional enzyme (MFE). Thus, disrupting or eliminating the functionality of MFE could halt the entire  $\beta$ -oxidation process [11]. The engineering of these genes may affect the absorption and utilization of lipid substrates by *Y. lipolytica*, thereby facilitating rapid growth and optimized lipid utilization.

In this study, an integrated strategy that consisted of creating modules for the enhancement of lipid uptake, accumulation and metabolism was used to systematically promote growth and lipid utilization in the commonly used *Y. lipolytica* Po1f strain (Fig. 1). Specifically, *Y. lipolytica* yDTY214 had an increased growth rate and greater lipid content, with a specific growth rate of  $0.32\text{ h}^{-1}$  and a lipid content of 67.66 % (g/g DCW), which were 54 % and 26 % greater than those of the original strain yDTY201, respectively. Finally,  $\beta$ -carotene served as an output to evaluate the bioproduction efficiency of the engineered strain, which achieved efficient utilization of the substrate and significantly reduced the time needed for  $\beta$ -carotene production to reach its peak. The knowledge gained by studying the effects of the hydrophobic substrate supply on cell growth, metabolic synergistic utilization, and  $\beta$ -carotene production will aid in the development of economically viable biosynthetic methods for lipid-to-terpenoid production.

## 2. Materials and methods

### 2.1. Yeast strains and culture

*E. coli* TOP10 was used for plasmid construction and subsequent amplification. *Y. lipolytica* Po1f (ATCC MYA-2613) was provided by Dr. Yongkun Lv (Zhengzhou University). All strains in this study are listed in Table 1.

*E. coli* strains were cultured in lysogeny broth (LB) on agar plates supplemented with 100  $\mu\text{g/mL}$  ampicillin. Yeast peptone dextrose (YPD) medium was formulated with 20 g/L peptone, 20 g/L glucose, and 10 g/L yeast extract. Yeast peptone oleic acid (YPO) medium was prepared with 20 g/L oleic acid instead of glucose and was used for fermentation of the engineered strains, and 1 % Tween 80 was added as a surfactant to promote the utilization of oleic acid. SC dropout medium enriched with the relevant specific amino acids was used for the selection of recombinant strains.

### 2.2. Plasmid construction and DNA manipulation

The BM Seamless Cloning Kit from Biomed Co., Ltd. (Beijing, China) was used to construct plasmids, which were subsequently transformed into *Y. lipolytica* strains with the Frozen-FZ yeast transformation IITM Kit from Zymo Research (USA). The plasmids and primers utilized in this study are outlined in Table 1 and Table S1. Furthermore, the relevant endogenous genes for this research were amplified from the genomic DNA of *Y. lipolytica* Po1f by PCR.

### 2.3. Assay of promoter strength

The strengths of the *POX2* and *LIP2* promoters were characterized via fluorescence intensity measurements of the red fluorescence protein DsRed. Following a 6-h cultivation in YPO medium, the cells were collected, rinsed, and diluted with phosphate-buffered saline to an OD<sub>600</sub> value ranging from 0.3 to 0.4 for fluorescence analysis. To quantify DsRed fluorescence, black microplates (Microfluor™) were employed along with a Varioskan LUX Multimode Microplate Reader (Thermo Scientific™), with the excitation and emission wavelengths precisely set at 510 nm and 590 nm, respectively. The strength of each promoter was evaluated by calculating the ratio of the promoter

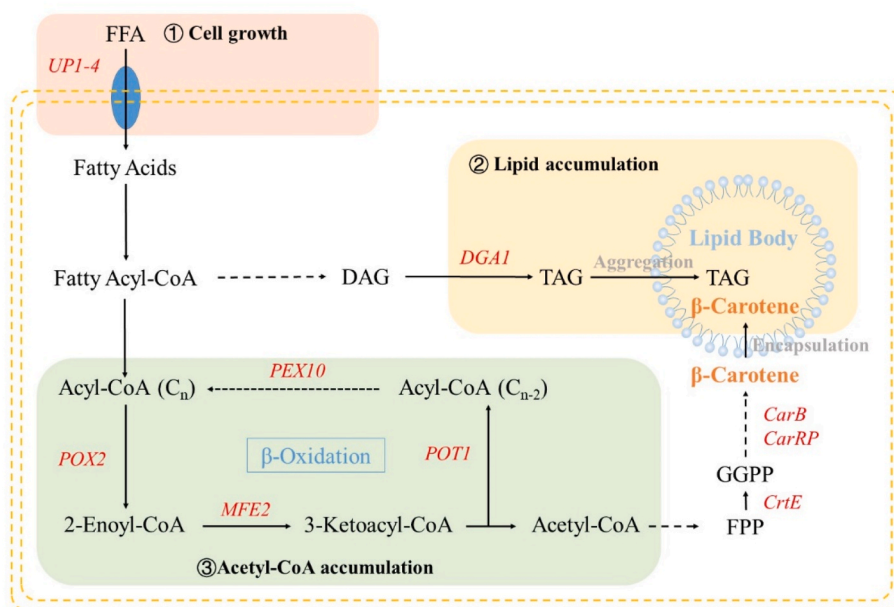


Fig. 1. Flowchart of the development of a rapid growing *Y. lipolytica* strain.

**Table 1**  
Strains and plasmids used in this study.

| Strain or plasmid         | Relevant properties or genotype   | Source     |
|---------------------------|---|------------|
| <b>Strains</b>            |   |            |
| <i>E. coli</i> TOP10      | F <sup>-</sup> , mcrAΔ(mrr-hsdRMS-mcrBC), φ80, lacZΔM15, ΔlacX74, recA1, araΔ139Δ(ara-leu)7697, galU, galK, rpsL <sub>2</sub> (str <sup>R</sup> ), endA1, nupG  | Biomed     |
| <i>Y. lipolytica</i> Po1f | MataA, ura3-302, leu2-270, xpr2-322, axp-2  | ATCC       |
| yDTY201                   | <i>Y. lipolytica</i> Po1f, ΔIntA::P <sub>EXPI</sub> -ERG20-T <sub>XPR2</sub> -P <sub>FBA1in</sub> -HMG1-T <sub>CYCI</sub> -P <sub>EXPI</sub> -HMG1-T <sub>XPR2</sub> , ΔIntC::P <sub>hp8d</sub> -ERG8-T <sub>XPR2</sub> -P <sub>FBA1in</sub> -ERG19-T <sub>CYCI</sub> -P <sub>EXPI</sub> -IDI-T <sub>XPR2</sub> , ΔIntE::P <sub>FBA1in</sub> -ERG12-T <sub>XPR2</sub> -P <sub>FBA1in</sub> -ERG10-T <sub>CYCI</sub> -P <sub>EXPI</sub> -ERG13-T <sub>T8</sub> | Our lab    |
| yDTY202                   | yDTY201, ΔIntB::P <sub>POX2p</sub> -DsRed-T <sub>T8</sub>   | This study |
| yDTY203                   | yDTY201, ΔIntB::P <sub>LIP2p</sub> -DsRed-T <sub>T8</sub>   | This study |
| yDTY204                   | yDTY201, ΔKu70::P <sub>LIP2p</sub> -UP1-T <sub>T8</sub>   | This study |
| yDTY205                   | yDTY201, ΔKu70::P <sub>LIP2p</sub> -UP2-T <sub>T8</sub>   | This study |
| yDTY206                   | yDTY201, ΔKu70::P <sub>LIP2p</sub> -UP3-T <sub>T8</sub>   | This study |
| yDTY207                   | yDTY201, ΔKu70::P <sub>LIP2p</sub> -UP4-T <sub>T8</sub>   | This study |
| yDTY208                   | yDTY201, ΔKu70::P <sub>LIP2p</sub> -UP1-T <sub>T8</sub> -P <sub>LIP2p</sub> -UP4-T <sub>T8</sub>  | This study |
| yDTY209                   | yDTY201, ΔIntD::P <sub>LIP2p</sub> -DGA1-T <sub>T8</sub> -P <sub>LIP2p</sub> -SCD-T <sub>T8</sub>   | This study |
| yDTY210                   | yDTY201, ΔKu80::P <sub>LIP2p</sub> -MFE2-T <sub>T8</sub>  | This study |
| yDTY211                   | yDTY201, ΔKu80::P <sub>LIP2p</sub> -POT1-T <sub>T8</sub>  | This study |
| yDTY212                   | yDTY201, ΔKu80::P <sub>LIP2p</sub> -PEX10-T <sub>T8</sub>   | This study |
| yDTY213                   | yDTY201, ΔKu80::P <sub>LIP2p</sub> -POX2-T <sub>T8</sub>  | This study |
| yDTY214                   | yDTY201, ΔKu70::P <sub>LIP2p</sub> -UP1-T <sub>T8</sub> -P <sub>LIP2p</sub> -UP4-T <sub>T8</sub> , ΔIntD::P <sub>LIP2p</sub> -DGA1-T <sub>T8</sub> -P <sub>LIP2p</sub> -SCD-T <sub>T8</sub> , ΔKu80::P <sub>LIP2p</sub> -MFE2-T <sub>T8</sub>   | This study |
| yDTY215                   | yDTY201, ΔIntF::P <sub>TEF1in</sub> -Mc_CarB-T <sub>CYCI</sub> -P <sub>EXPI</sub> -Mc_CarRP-T <sub>T8</sub> -P <sub>FBA1in</sub> -Tm_CrtE-T <sub>T8</sub>   | This study |
| yDTY216                   | yDTY214, ΔIntF::P <sub>TEF1in</sub> -Mc_CarB-T <sub>CYCI</sub> -P <sub>EXPI</sub> -Mc_CarRP-T <sub>T8</sub> -P <sub>FBA1in</sub> -Tm_CrtE-T <sub>T8</sub>   | This study |
| <b>Plasmids</b>           |   |            |
| pYRSB                     | IntB site deletion cassette in pUC57  | Our lab    |
| pYRSB                     | IntD site deletion cassette in pUC57  | Our lab    |
| pYRSF                     | IntF site deletion cassette in pUC57  | Our lab    |
| pYRS70                    | Ku70 deletion cassette in pUC57   | Our lab    |
| pYRS80                    | Ku80 deletion cassette in pUC57   | Our lab    |
| pDTY201                   | P <sub>POX2p</sub> -DsRed-T <sub>T8</sub> cassette in pYRSB   | This study |
| pDTY202                   | P <sub>LIP2p</sub> -DsRed-T <sub>T8</sub> cassette in pYRSB   | This study |
| pDTY203                   | P <sub>LIP2p</sub> -UP1-T <sub>T8</sub> cassette in pYRS70  | This study |
| pDTY204                   | P <sub>LIP2p</sub> -UP2-T <sub>T8</sub> cassette in pYRS70  | This study |
| pDTY205                   | P <sub>LIP2p</sub> -UP3-T <sub>T8</sub> cassette in pYRS70  | This study |
| pDTY206                   | P <sub>LIP2p</sub> -UP4-T <sub>T8</sub> cassette in pYRS70  | This study |
| pDTY207                   | P <sub>LIP2p</sub> -UP1-T <sub>T8</sub> -P <sub>LIP2p</sub> -UP4-T <sub>T8</sub> cassette in pYRS70   | This study |
| pDTY208                   | P <sub>LIP2p</sub> -DGA1-T <sub>T8</sub> -P <sub>LIP2p</sub> -SCD-T <sub>T8</sub> cassette in pYRSB   | This study |
| pDTY209                   | P <sub>LIP2p</sub> -MFE2-T <sub>T8</sub> cassette in pYRS80   | This study |
| pDTY210                   | P <sub>LIP2p</sub> -POT1-T <sub>T8</sub> cassette in pYRS80   | This study |
| pDTY211                   | P <sub>LIP2p</sub> -PEX10-T <sub>T8</sub> cassette in pYRS80  | This study |
| pDTY212                   | P <sub>LIP2p</sub> -POX2-T <sub>T8</sub> cassette in pYRS80   | This study |
| pDTY213                   | P <sub>TEF1in</sub> -Mc_CarB-T <sub>CYCI</sub> -P <sub>EXPI</sub> -Mc_CarRP-T <sub>T8</sub> -P <sub>FBA1in</sub> -Tm_CrtE-T <sub>T8</sub> cassette in pYRSF   | This study |

fluorescence intensity to the OD<sub>600</sub> value for each individual strain.

#### 2.4. Growth curve determination

Inoculation of cells that were cultivated overnight in YPO medium, was carried out at an initial OD<sub>600</sub> of 0.5, with three biological replicates. Biomass production was subsequently monitored by measuring the OD<sub>600</sub> values at regular intervals of 2 to 3 h. The cells cultured with oleic acid were washed twice with a 0.5 % solution of bovine serum albumin, followed by a single wash with 0.9 % saline, prior to the OD<sub>600</sub> measurement [12].

#### 2.5. Nile red staining

DIC and fluorescence images were captured at 1000× oil immersion magnification using an OLYMPUS BX53 upright microscope. The cells were stained with Nile red dye at a concentration of 0.1 mg/L for 5 min. The sample emitted red fluorescence at an excitation wavelength of 552 nm.

#### 2.6. Metabolite quantification

For the detection of oleic acid in YPO culture medium, 200 μL of cells were mixed with 300 μL of KOH-methanol solution and incubated at 65 °C for 2 h for methyl esterification. A total of 450 μL of n-hexane was added, and the mixture was vortexed for 10 min for extraction; this process was repeated 2 times. The extract was collected and dried under a vacuum, dissolved in 300 μL of n-hexane and used for GC-MS analysis.

To extract fatty acids, the strains were cultivated using identical media and conditions to those used for the growth curve experiments. This process was performed with three biological replicates. At three distinct growth stages, yeast cell samples were collected and centrifuged at 4000 rpm for 5 min. The resulting cell pellets underwent a two-step washing process: first, half the volume of 0.5 % bovine serum albumin was added, followed by a rinse with half the volume of 0.9 % saline. The cells were subsequently dried under a vacuum for 12–20 h until they were powdered. The next step involved adding 1 mL of 3 N HCl-methanol solution and 100 μL of chloroform, followed by incubation at 70 °C for 3 h. After cooling to room temperature, a few NaCl particles were introduced, and the mixture was vortexed for 15 s. Then, 1 mL of n-hexane was added, the mixture was vortexed for 20 min and centrifuged to separate the organic phase for further analysis using GC-MS.

Fatty acid methyl esters (FAMES) were separated and analyzed via a GCMS-QP2020 system (SHIMADZU, Japan) with a DB-5MS column (30 m × 0.25 mm × 0.25 μm, J&W Scientific, CA). The initial temperature was 70 °C for 5 min, and the temperature was increased to 300 °C at 10 °C/min for 3 min. FAME concentrations were quantified through the utilization of a 37-component FAME mix standard from Sigma-Aldrich. The level of acetyl-CoA was detected via an A-CoA ELISA Kit purchased from Zeye Biotechnology Co., Ltd. (Shanghai, China).

#### 2.7. Genes transcriptional analysis

Relative expression levels of modified genes in this study were analyzed by Quantitative Real-Time PCR (qPCR). Strains were cultured in shake flasks and harvested at three distinct growth stages. Total RNA extraction, reverse transcription, and qPCR were carried out by Tsingke Inc. (China). The gene *actin1* was used for normalization.

#### 2.8. β-Carotene fermentation and determination

For β-carotene fermentation, a colony was seeded on agar plates in YPD medium and incubated overnight. This colony was subsequently transferred to YPO media for scaled-up cultivation. The cells were grown under continuous agitation at 220 rpm and 28 °C for a total duration of 96 h, culminating in the harvesting of the fermentation product.

$\beta$ -Carotene extraction from the strains was achieved through acid treatment [13]. First, harvested cells were rinsed with ddH<sub>2</sub>O and suspended in 3 N HCl. The cells were lysed by boiling the solution. Next, the cellular debris was washed twice with ddH<sub>2</sub>O and resuspended in acetone containing 1 % (w/v) butylated hydroxytoluene. To facilitate further extraction, glass beads were added, and the mixture was vortexed until it turned white. Finally, the acetone phase was separated by centrifugation and filtered through 0.22  $\mu$ m organic membranes for HPLC analysis.

$\beta$ -Carotene analysis and quantification were performed with a SHIMADZU SPD-20A system equipped with a BDS Hypersil C18 column (Thermo Scientific) for UV detection. The mobile phase was composed of a mixture of acetonitrile:water (9:1 v/v) and methanol:isopropanol (3:2 v/v) and was mixed at a rate of 1 mL/min at 25 °C.  $\beta$ -Carotene standards were sourced from Sigma-Aldrich.

3. Results and discussion

3.1. Rapid import of extracellular free fatty acids

*Y. lipolytica* was renowned for its ability to metabolize hydrophobic substrates, including methyl oleate [14] and oleic acid [15]. Oleic acid was used as the substrate in this study to investigate the lipid utilization efficiency of *Y. lipolytica*. The promoters *POX2p* and *LIP2p* are commonly used oleic acid-inducible promoters that have been successfully used to drive gene expression [16]. To identify the promoter that exhibited a heightened response to oleic acid, the DsRed fluorescent protein was used to assess the induction levels of *POX2p* in strain yDTY202 (*POX2p*-DsRed) and *LIP2p* in strain yDTY203 (*LIP2p*-DsRed), both of which were cultivated in YPO medium. Fig. 2A depicts the specific fluorescence, which was corrected for biomass. In YPO medium supplemented with oleic acid as the carbon source, *LIP2p* induction surpassed that of *POX2p*, which aligns with previous findings that suggest that *LIP2p* was the preferred promoter for the production of recombinant proteins [16]. Therefore, the *LIP2p* promoter was selected for

gene expression in this study.

In the metabolic pathway of hydrophobic substrates, the initial stage involves their translocation into the cell. Previous studies have suggested intriguing possibilities regarding the potential involvement of the YIUP1p-UP4p transporter family in the intricate process of extracellular fatty acid import in *Y. lipolytica*. These studies suggest that these proteins play critical roles in facilitating the efficient translocation of fatty acids across the cell membrane, thereby enabling the yeast to harness these valuable nutrients from its external environment. The proposed function of YIUP1p-UP4p as a fatty acid importer underscores its importance in maintaining the metabolic balance and growth performance of *Y. lipolytica*, as well as its potential for use in biotechnology applications aimed at increasing lipid production and improving metabolic engineering strategies [8]. However, the precise mechanism of action of both the individual genes belonging to the YIUP1p-UP4p family and the combination of those genes, remains to be elucidated. In this study, the *LIP2p* promoter was utilized to express the *UP1–UP4* genes, and the yDTY204-yDTY207 strains were obtained. Analysis of the growth patterns of the cells cultured in YPO media revealed a noteworthy phenomenon: the overexpression of the *UP1–UP4* gene family significantly increased the specific growth rate of the yeast. Specifically, *UP4* was a particularly potent enhancer, increasing the growth rate of the control strain yDTY201 from a baseline of 0.22–0.28 (Fig. 2B). This enhancement underscores the pivotal role that *UP4*, and potentially the entire *UP1–UP4* gene suite, plays in promoting cellular proliferation. Concurrently, the analysis revealed a favorable effect on two key metabolic parameters: the substrate consumption rate ( $Y_S$ ) and the growth yield ( $Y_{X/S}$ ). The increase in the  $Y_S$  signifies an increased capacity of the cells to efficiently utilize the available nutrients from the medium, whereas the increase in  $Y_{X/S}$  indicates a more productive conversion of these substrates into biomass (Fig. 2C). Thus, the overexpression of the *UP1–UP4* genes can increase the rate at which oleic acid was consumed, resulting in the production of more lipids. These findings collectively underscore the multifaceted benefits of *UP1–UP4* overexpression, not only in accelerating growth but also in optimizing metabolic processes

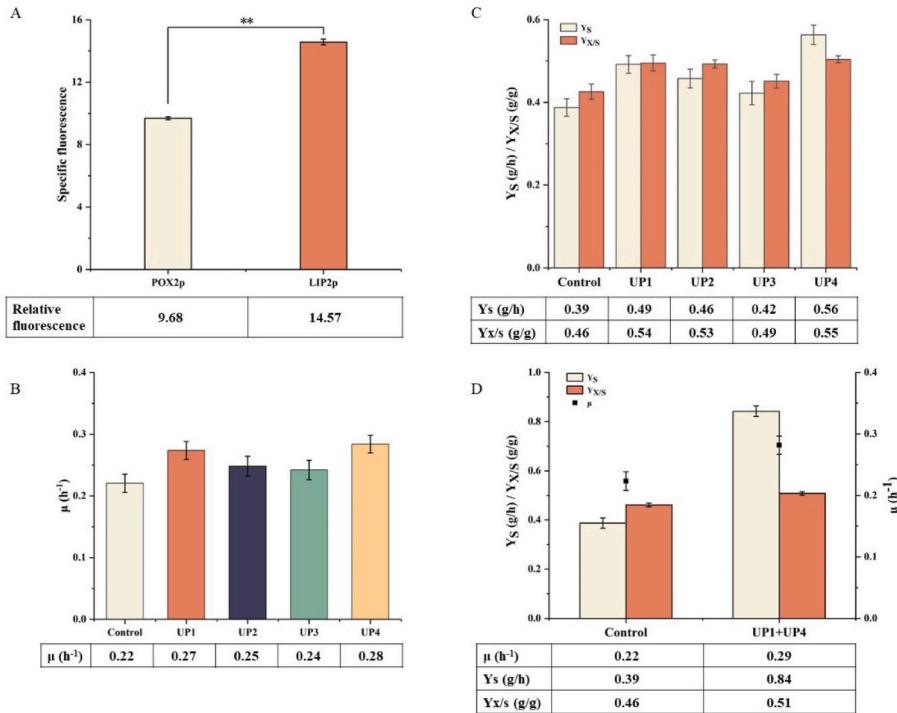


**Fig. 2.** Characterization of the cell growth module. (A) Relative fluorescence intensity of the *POX2* and *LIP2* promoters in oleic acid medium. (B) Specific growth rate  $\mu$  of strains expressing *UP1–UP4*. (C) rate  $Y_S$  and  $Y_{X/S}$  of strains expressing *UP1–UP4*. (D)  $\mu$ ,  $Y_S$  and  $Y_{X/S}$  of strains co-expressing *UP1* and *UP4*. The control refers to strain yDTY201.



that are essential for cellular fitness and productivity. The growth of strains co-expressing *UP1–UP4* was subsequently examined (Fig. S1), revealing that the co-expression of *UP1* and *UP4* increased the specific growth rate to  $0.29\text{ h}^{-1}$ . This combination further increased the substrate consumption rate ( $Y_s$ ) to 0.84 and the production yield ( $Y_{X/s}$ ) to 0.51 (Fig. 2D). qPCR results demonstrated that the relative expression of *UP1* increased mainly in the early stage of cell growth ( $1/5\text{ OD}_{\max}$ ), while the relative expression of *UP4* increased in the late stage ( $\text{OD}_{\max}$ ) (Table S4 and Fig. S6). The co-expression of *UP1* and *UP4* accelerated the absorption of extracellular fatty acids and constructed a rapid cell growth module. A previous study demonstrated that the role of *UP1* in the import of C10, C12, and C14 fatty acids. Despite the overexpression of *UP1* in a strain deficient in *UP1–4*, minimal growth was observed. Interestingly, *UP4* overexpression seemed to partly mitigate the growth inhibition by promoting the import of the medium-chain fatty acids mC12 and mC14, indicating their specific preference for these fatty acid types [8]. This study revealed that the overexpression of *UP1–4* has a positive effect on the utilization of C18 oleic acid, especially the simultaneous overexpression of *UP1* and *UP4*.

### 3.2. Increased lipid accumulation through the overexpression of *DGA1* and *SCD*

*Y. lipolytica* predominantly sequesters lipids within lipid bodies, which serve as the epicenter of lipid accumulation and energy homeostasis. These dynamic organelles primarily harbor intracellular neutral lipids, with triglycerides constituting 85 % of the lipid content [10]. Genes that increase lipid accumulation are well characterized and available for production [17,18]. By co-expressing diacylglycerol acyltransferase (*DGA1*) and delta-9 stearoyl-CoA desaturase (*SCD*), strain yDTY209 was successfully generated. The effects of *DGA1* and *SCD* overexpression on lipid production were evaluated through shake flask experiments (Fig. 3). To assess the maximum capacity for lipid storage, the cellular lipid content was analyzed at multiple intervals. From the growth curves, three specific time points were chosen, spanning from the early exponential phase to the plateau phase. The specific time points closely aligned with the one-fifth, half, and full maximum  $\text{OD}_{600}$  ( $\text{OD}_{\max}$ ) values (Fig. S2). For lipid extraction, cellular samples were collected from three biological replicates at approximately these three growth curve-derived time points. The lipid contents were subsequently quantified at three designated time points:  $1/5$ ,  $1/2$ , and  $1\text{ OD}_{\max}$ . As shown in Fig. 2A, the control strain had a lipid content of 51.99 % (g/g DCW) at the highest point ( $1/2\text{ OD}_{\max}$ ), exhibiting comparable performance to that of wild-type strains cultured with oleic acid as the carbon source [15]. The relative expression levels of *DGA1* and *SCD* increased during the whole period (Table S4 and Fig. S6). Co-expression of *DGA1* and *SCD* increased the lipid content to 60.37 % (g/g DCW) at the same

time point. In the two strains, the accumulation of C12–C18 compounds was prominent, with the increase in lipid content attributed to the combined effects of C16:0 and C18:2 fatty acid (Fig. S3). Intracellular staining for triacylglycerols (TAGs) and subsequent imaging analysis of yDTY201 and yDTY209 (Fig. 3B and C) showed an increased in lipid body volume and lipid accumulation.

The importance of *DGA1* in promoting growth and lipid synthesis has been underscored. In the yeast *Y. lipolytica*, the trio of acyltransferases—*DGA1*, *DGA2*, and *PDAT*—orchestrate the culminating step of converting diacylglycerol to TAG. Eliminating these acyltransferases simultaneously leads to pronounced impairments in the lag phase as well as the growth rate, thereby implying an intricate link between oil biosynthesis and healthy growth [19]. With the aim of increasing lipid accumulation, a strategic dual-overexpression approach was implemented to target both the *DGA1* and *ACC1* genes in *Y. lipolytica*. This innovative genetic manipulation led to a remarkable increase in the lipid content, resulting in a substantial increase to 41.4 % of the total dry cell weight (DCW) [18]. Notably, *SCD* emerged as a pivotal metabolic regulatory enzyme that catalyzes the  $\Delta 9$  desaturation of palmitoyl-CoA and stearoyl-CoA to palmitoleoyl-CoA and oleoyl-CoA, respectively. When *SCD* was overexpressed, the fatty acid biosynthesis pathway was activated, and the inhibitory effects of two intermediates in the pathway, palmitoyl-CoA and stearoyl-CoA, on *ACC1* were effectively relieved. Consequently, the alleviation of these inhibitory increases the efficiency of fatty acid biosynthesis, ultimately enhancing the lipid production capabilities of *Y. lipolytica* [9]. When *DGA1* was concurrently activated alongside *SCD*, a harmonious interplay ensues, facilitating a delicately balanced redirection of carbon flux toward TAG production. This orchestrated process not only optimizes the overall yield of TAG but also effectively minimizes the accumulation of intermediate metabolites, which could impede the efficiency of the lipid synthesis pathway by exerting inhibitory effects. By maintaining this fine balance, the system ensures that resources are allocated efficiently and that production proceeds smoothly. In summary, the co-expression of *DGA1* and *SCD* greatly increases the volume of the lipid body, allowing the fatty acids absorbed into the cells to be efficiently utilized and building a lipid accumulation module.

### 3.3. Regulating $\beta$ -oxidation to increase the acetyl-CoA supply

Once internalized and activated, fatty acids are metabolized via  $\beta$ -oxidation or  $\omega$ -oxidation.  $\beta$ -Oxidation is preferred because of its energetic efficiency and is crucial for acetyl-CoA production when fats are the primary carbon source [10,20]. Therefore, to obtain a sufficient supply of acetyl-CoA, we overexpressed four key genes in the  $\beta$ -oxidation pathway, including *MFE2*, *POT1*, *PEX10* and *POX2*. Results showed the overexpression of *MFE2* significantly increased the acetyl-CoA level

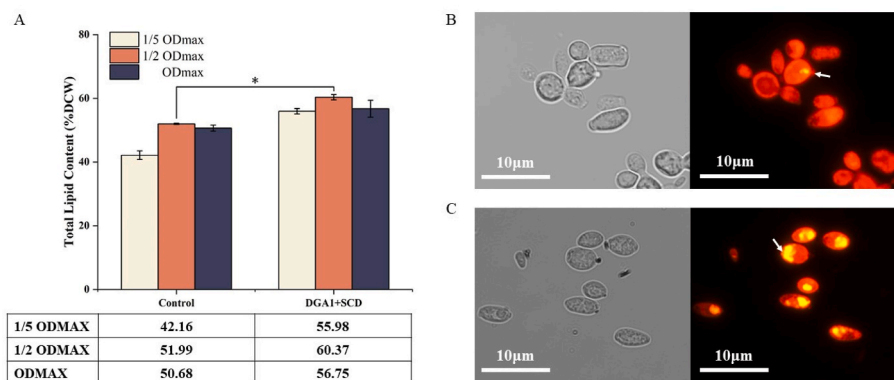


**Fig. 3.** Characterization of the lipid accumulation module. (A) Lipid contents of the control yDTY201 and yDTY209 strains in shaking flask cultures. Differential interference contrast microscopic and fluorescence microscopy images of (B) control yDTY201 cells and (C) yDTY209 cells containing *DGA1* and *SCD*. All the cells were stained with Nile red before being viewed under a fluorescence microscope along with DIC imaging. The scale bars represent 10  $\mu\text{m}$ .

by 52 %, from 1.88 ng/L/OD to 2.87 ng/L/OD (Fig. 4).

For medium- and long-chain fatty acids, degradation typically occurs via  $\beta$ -oxidation in peroxisomes following their activation [10]. Among them, *MFE2*, a critical enzyme in the  $\beta$ -oxidation pathway, is integral to fatty acid metabolism. Mutations or deletions in *MFE2* impede  $\beta$ -oxidation. This specific approach has garnered considerable attention in lipid production research, owing to its simplicity compared with deleting six *POX* genes [11]. Deleting the *MFE2* gene increases pentane production, mainly because of its ability to promote lipid accumulation and specifically increase linoleic acid content [21]. In essence, the overexpression of the *MFE2* gene elicited a multifaceted response within the cellular machinery, resulting in a substantial increase in the intracellular content of acetyl-CoA [22–24]. This augmented pool of acetyl-CoA, a crucial metabolic intermediate, subsequently serves as a potent activator of the  $\beta$ -oxidation pathway, initiating a cascade of enzymatic reactions that facilitate the efficient breakdown of fatty acids. Furthermore, this orchestrated process effectively constructed an acetyl-CoA accumulation module, which was a dynamic system that not only enhances the retention of this valuable metabolite but also positions it as a pivotal hub for various biosynthetic and catabolic pathways, thereby broadening the metabolic versatility and capabilities of *Y. lipolytica*.

### 3.4. Integration of modules for efficient utilization of lipids

Previously, we screened the optimal genes for each module by co-expressing *UP1* and *UP4*, *DGA1* and *SCD*, and *MFE2*. Next, we integrated the overexpression plasmid pDTY207-pDTY209 with the three modules into the control strain yDTY201 to obtain strain yDTY214. When cultured in the same YPO medium, the specific growth rate of strain yDTY214 increased to  $0.32 \text{ h}^{-1}$ , which was 45.4 % greater than that of the control yDTY201 ( $0.22 \text{ h}^{-1}$ ) (Fig. 5A). The observed specific growth rate of the control strain yDTY201 in oleic acid-containing medium was comparable to that reported in previous studies, indicating that the experimental conditions effectively supported the proliferation of this yeast strain utilizing oleic acid as the sole carbon source [15,25]. This similarity underscores the consistency and reproducibility of *Y. lipolytica* growth behavior in oleic acid media across different experimental setups and conditions. Moreover, the substrate consumption rate and growth yield also increased to 0.48 g/h and 0.68 g/g, respectively. Co-expression of *UP1* and *UP4* may accelerate the transport

of extracellular fatty acids into the cell, and cells can quickly utilize substrates to increase biomass and achieve rapid cell growth.

The total lipid content of strain yDTY214 reached 67.66 % (g/g DCW) ( $1/2 \text{ OD}_{\text{max}}$ ), which was also clearly observed in the Nile red staining images of intracellular lipids (Fig. 5C and D). The lipid accumulation of strain yDTY201 was similar to that of wild-type strain Po1f, demonstrating that modification of the MVA pathway did not significantly change fatty acid accumulation (Table S3 and Fig. S4). On the contrary, all the other genetic modification involved in this study significantly increased lipid accumulation, mainly as saturated fatty acids (including saturated fatty acids C12, C16 and C18, Fig. S5). Notably, the co-expression of *DGA1* and *SCD* most notably increasing the ratio of unsaturated fatty acid C18:2. The proportion of unsaturated fatty acid C18:2 in strain yDTY214 was 22.73 % higher than that in strain yDTY201 at the time point  $1/2 \text{ OD}_{\text{max}}$ . It has been reported that upregulation of *SCD* effectively increased the relative abundance of unsaturated fatty acids in yeast cells and would enhance cellular tolerance to various stresses [26,27]. That might have explained the reason why the specific growth rate of strain yDTY214 ( $0.32 \text{ h}^{-1}$ ) is higher than that of yDTY208 ( $0.29 \text{ h}^{-1}$ ). *DGA1* contribute distinctly to the modulation of lipid storage processes and have beneficial effects particularly on the accumulation of hydrophobic terpenoids [28,29]. In conclusion, concurrent overexpression of *DGA1* and *SCD* notably increased the liposome volume, enabling proficient harnessing of intracellular fatty acids and modulating the levels of their unsaturated forms.

The acetyl-CoA content of strain yDTY214 increased to 3.42 ng/L/OD, which was 82 % greater than that of the control (1.88 ng/L/OD) (Fig. 5B). At the same time, the relative expression level of *MFE2* significantly increased in the late stage of cell growth ( $\text{OD}_{\text{max}}$ ) (Table S4 and Fig. S6), which can increase the accumulation of acetyl-CoA in the product synthesis stage, providing important precursors for various downstream biological products [30]. Research has demonstrated that the overexpression of *MFE2* in *Y. lipolytica* increases the acetyl-CoA content, facilitating ample precursor availability for amorphadiene biosynthesis [31]. In parallel, elevated *MFE2* expression may create additional  $\beta$ -oxidation sites, enabling the efficient synthesis of acetyl-CoA from these fatty acids.

The aforementioned findings conclusively demonstrate the successful acquisition of a genetically engineered *Y. lipolytica* strain, designated yDTY214, which has remarkable capabilities. This recombinant strain exhibits exceptional proficiency in efficiently harnessing oils as a primary carbon and energy source, leading to notable enhancements in its growth kinetics. Specifically, yDTY214 undergoes rapid cell proliferation, which is indicative of its robust metabolic fitness and adaptability. Additionally, this strain is adept at swiftly accumulating lipids and acetyl-CoA, two vital metabolic intermediates that play pivotal roles in various biosynthetic and catabolic pathways. This dual capacity for rapid growth and metabolite accumulation underscores the transformative potential of the yDTY214 strain and its potential applications in biotechnology and industrial fermentation processes.

### 3.5. Natural product output of fast-growing strains

$\beta$ -Carotene, a naturally occurring lipophilic compound, has been extensively applied as an additive across diverse industries, such as the food, textile, chemical, and cosmetic industries. Its widespread acceptance is attributed to its health benefits, red-to-yellow pigmentation, and GRAS status [32]. Additionally,  $\beta$ -carotene possesses antioxidant properties and serves as a precursor for the synthesis of numerous carotenoid-based drugs [28]. Owing to its distinct color, it can serve as a model for studying microbial natural product synthesis [33]. Since  $\beta$ -oxidation of fatty acids generates acetyl-CoA, the key building block for terpene synthesis via the natural mevalonate pathway, *Y. lipolytica* can function as a lipid-to-terpenoid platform [34]. An engineered strain of *Y. lipolytica* exhibited remarkable  $\beta$ -carotene production, achieving a yield of 39.5 g/L in fed-batch bioreactor fermentations [7]. Although the

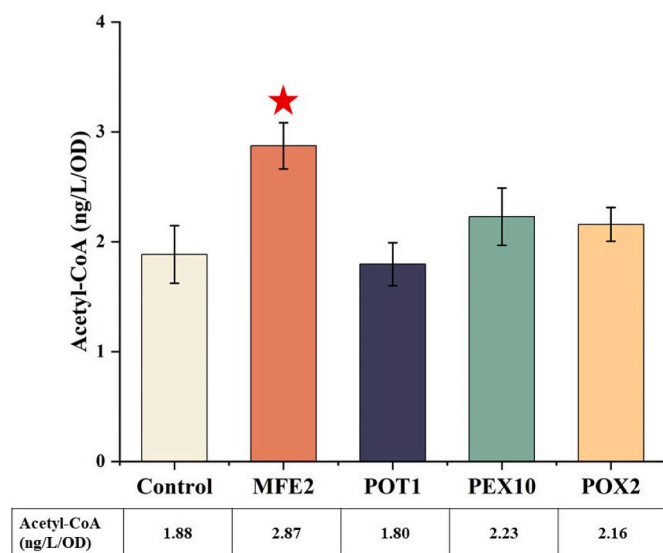
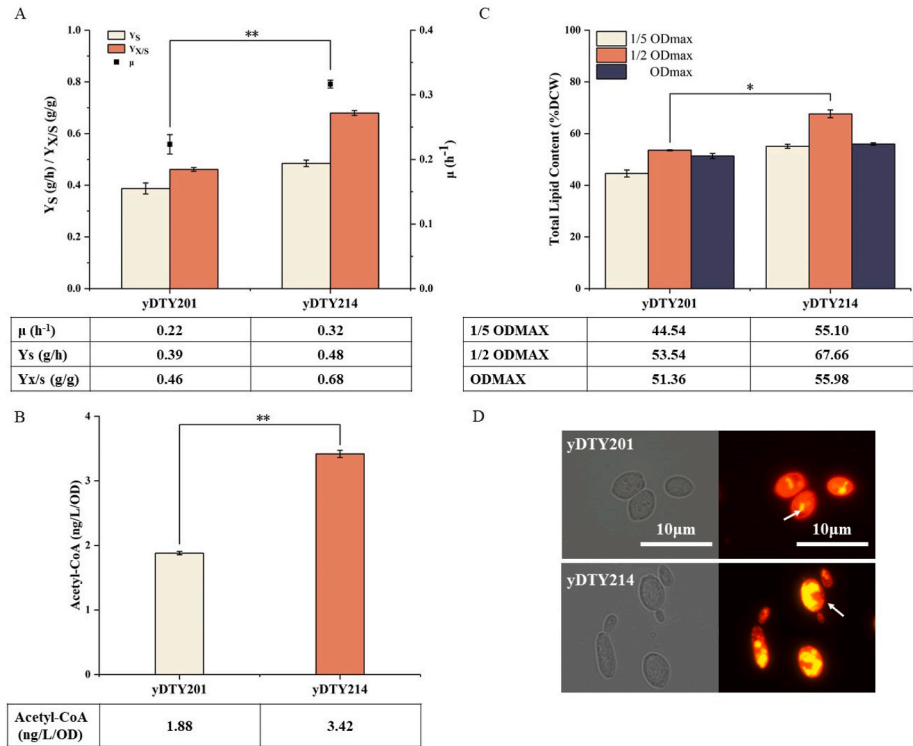


Fig. 4. Characterization of the acetyl-CoA accumulation module. Effect of acetyl-CoA content in strains expressing  $\beta$ -oxidation genes, including *MFE2*, *POT1*, *PEX10* and *POX2*. The control refers to strain yDTY201.



**Fig. 5.** Characterization of the lipid utilization effects of the integrated three-module strain yDTY214 and the control strain yDTY201. (A)  $\mu$ ,  $Y_s$   $Y_{x/s}$ . (B) Acetyl-CoA content. (C) Lipid contents. (D) Fluorescence microscope image after Nile red staining. The scale bars represent 10  $\mu\text{m}$ .

yield was high, the fermentation cycle was very long (240 h). To solve the problem of a long yeast fermentation cycle, we generated a strain with efficient oil utilization and tested its ability to produce large amounts of  $\beta$ -carotene.

*CarB* and *CarRP* derived from *Mucor circinelloides* and *CrtE* derived from *Taxus x media* ( $\beta$ -carotene synthesis module) were integrated into strain yDTY214 to obtain yDTY216. The  $\beta$ -carotene synthesis module was also integrated into the control to obtain strain yDTY215.  $\beta$ -Carotene production was determined in YPO media supplemented with 2 % oleic acid. The results revealed that strain yDTY216 rapidly accumulated  $\beta$ -carotene during the logarithmic growth phase, and the biomass growth rate was also significantly greater than that of the control (Fig. 6A). Within the same fermentation time (48 h), strain yDTY216 can produce more  $\beta$ -carotene with less raw material, which is nearly double that of the control strain yDTY215, and the speed of product synthesis becomes faster. During the fermentation experiments conducted with the yDTY215 strain, a discernible transformation occurred within the cellular landscape. Specifically, lipid droplets, which are initially dispersed throughout the cytoplasm, undergo a progressive

agglomeration process, ultimately coalescing into lipid bodies. This aggregation served as a crucial step in the sequestration and containment of the newly synthesized  $\beta$ -carotene, effectively isolating it within the confines of these lipid bodies during the initial 48 h of fermentation (Fig. 6B). As the fermentation process progresses toward its latter stages, the lipid bodies become increasingly difficult to discern, primarily because of the breakdown of these TAGs. This metabolic shift led to a more widespread and dispersed distribution of accumulated  $\beta$ -carotene throughout the intracellular environment. Compared to the yDTY215 strain, the yDTY216 strain presented a distinct metabolic profile characterized by a heightened rate of extracellular fatty acid absorption and accelerated lipid accumulation. As a result, even during the later stages of fermentation, lipid bodies remained conspicuously visible, providing ample additional space for the accumulation of  $\beta$ -carotene. This unique capacity for lipid storage not only facilitated the sequestration of  $\beta$ -carotene but also potentially enhanced its overall production and stability within the cellular environment (Fig. 6B). During the stationary phase of growth, strain yDTY216 exhibited a metabolic adaptation that involved TAG degradation. This process, which was primarily mediated

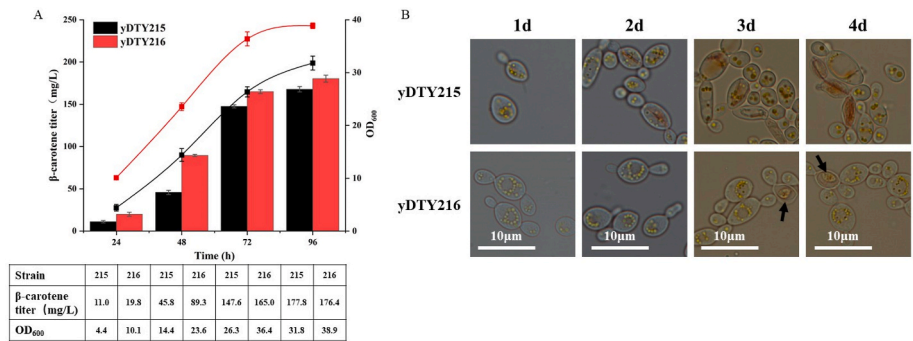


**Fig. 6.** Verification of the ability of the efficient oil utilization strain yDTY215 and the control strain yDTY216 to produce  $\beta$ -carotene. (A)  $\beta$ -carotene titer and biomass. (B) Microscopy image of cells during the  $\beta$ -carotene fermentation cycle. Three independent experiments were repeated with similar results.



through  $\beta$ -oxidation, resulted in the generation of acetyl-CoA, a key metabolic intermediate. By harnessing this pathway, the strain was able to replenish its pool of carbon skeletons, which subsequently served as building blocks for the increased synthesis of  $\beta$ -carotene. Therefore, strain yDTY216 demonstrated a remarkable ability to optimize its metabolic resources and maximize the production of this valuable carotenoid. Moreover, strain yDTY216 demonstrated remarkable proficiency in efficiently harnessing lipid substrates as a source of energy and carbon, resulting in a significant increase in metabolic efficiency. This optimized utilization of available resources not only facilitated the rapid progression of cellular processes but also led to a notable reduction in the overall fermentation cycle duration. Specifically, the product accumulation rate of strain yDTY216 (2.90 mg/L/h) was twice that of strain yDTY215 (1.45 mg/L/h), highlighting the strain's capacity for accelerated  $\beta$ -carotene production and increased productivity. The expedited growth of the chassis effectively reduces the fermentation period while increasing the yield of the target product. Additionally, researchers have devised a cell growth model rooted in coarse-grained proteome partitioning for rapidly proliferating bacteria. Their findings revealed that the coordinated regulation of ribosome- and tRNA-associated proteins aligns with the observed growth rate dependencies, leading to near-optimal resource allocation across diverse growth rates [35]. Through a combination of gene knockout and adaptive evolution, the highly efficient strain of *B. subtilis* A4003 was engineered to exhibit an exceptional specific growth rate of  $0.75\text{ h}^{-1}$  in M9 medium, surpassing that of the original strain by a remarkable percentage of 54.69 %. This rapidly growing strain shows great potential for increasing valuable compound and heterologous protein production, exemplified by its ability to produce RNA, acetoin, GFP, and ovalbumin [36].

#### 4. Conclusions

In this study, the co-expression of *UP1* and *UP4* promotes fatty acid absorption, the co-expression of *DGA1* and *SCD* enhances lipid accumulation, and the overexpression of *MFE2* increases the acetyl-CoA pool, resulting in efficient utilization of hydrophobic substrates by *Y. lipolytica*. A recombinant *Y. lipolytica* strain that can efficiently utilize oil was obtained, and the duration of the fermentation process for  $\beta$ -carotene production was significantly reduced, decreasing from an initial 96 h to an efficient 48 h. This study has great potential for increasing the synthesis rate of lipophilic natural products and provides new ideas for the development of economically viable biosynthetic methods for lipid-to-terpenoid production.

#### CRedit authorship contribution statement

**Tianyu Dong:** Writing – original draft, Methodology, Investigation, Data curation. **Yujie Shu:** Methodology, Data curation. **Ying Wang:** Writing – review & editing, Supervision. **Mingdong Yao:** Writing – review & editing, Supervision. **Wenhai Xiao:** Writing – review & editing, Supervision, Project administration, Investigation, Funding acquisition, Conceptualization.

#### Declaration of competing interest

The authors declare that they have no known competing financial interests or personal relationships that could have appeared to influence the work reported in this paper.

#### Acknowledgements

This work was supported by the National Key Research and Development Program of China (2021YFC2101000). This work was also supported by the Key-Area Research and Development Program of Guangdong Province (2020B0303070002) and the National Natural Science Foundation of China (22178261). The authors would like to

thank Dr. Yongkun Lv from the Zhengzhou University for kindly providing the *Y. lipolytica* Po1f (ATCC MYA-2613).

#### Appendix A. Supplementary data

Supplementary data to this article can be found online at <https://doi.org/10.1016/j.synbio.2025.01.007>.

#### References

- [1] Soong YV, Liu N, Yoon S, Lawton C, Xie D. Cellular and metabolic engineering of oleaginous yeast *Yarrowia lipolytica* for bioconversion of hydrophobic substrates into high-value products. *Eng Life Sci* 2019;19:423–43. <https://doi.org/10.1002/elsc.201800147>.
- [2] Soong YV, Zhao L, Liu N, Yu P, Lopez C, Olson A, Wong HW, Shao Z, Xie D. Microbial synthesis of wax esters. *Metab Eng* 2021;67:428–42. <https://doi.org/10.1016/j.ymben.2021.08.002>.
- [3] Xu M, Yang N, Pan J, Hua Q, Li CX, Xu JH. Remodeling the homologous recombination mechanism of *Yarrowia lipolytica* for high-level biosynthesis of squalene. *J Agric Food Chem* 2024;72:9984–93. <https://doi.org/10.1021/acs.jafc.4c01779>.
- [4] Ren X, Liu M, Yue M, Zeng W, Zhou S, Zhou J, Xu S. Metabolic pathway coupled with fermentation process optimization for high-level production of retinol in *Yarrowia lipolytica*. *J Agric Food Chem* 2024;72:8664–73. <https://doi.org/10.1021/acs.jafc.4c00377>.
- [5] Abdel-Mawgoud AM, Markham KA, Palmer CM, Liu N, Stephanopoulos G, Alper HS. Metabolic engineering in the host *Yarrowia lipolytica*. *Metab Eng* 2018;50:192–208. <https://doi.org/10.1016/j.ymben.2018.07.016>.
- [6] Liu M, Wu J, Yue M, Ning Y, Guan X, Gao S, Zhou J. YaliCMulti and YaliHMulti: stable, efficient multi-copy integration tools for engineering *Yarrowia lipolytica*. *Metab Eng* 2024;82:29–40. <https://doi.org/10.1016/j.ymben.2024.01.003>.
- [7] Ma Y, Liu N, Greisen P, Li J, Qiao K, Huang S, Stephanopoulos G. Removal of lycopene substrate inhibition enables high carotenoid productivity in *Yarrowia lipolytica*. *Nat Commun* 2022;13:572. <https://doi.org/10.1038/s41467-022-28277-w>.
- [8] Onesime D, Vidal L, Thomas S, Henry C, Martin V, Andre G, et al. A unique, newly discovered four-member protein family involved in extracellular fatty acid binding in *Yarrowia lipolytica*. *Microb Cell Factories* 2022;21(1):200. <https://doi.org/10.1186/s12934-022-01925-y>.
- [9] Qiao K, Abidi SHI, Liu H, Zhang H, Chakraborty S, Watson N, Ajikumar PK, Stephanopoulos G. Engineering lipid overproduction in the oleaginous yeast *Yarrowia lipolytica*. *Metab Eng* 2015;29:56–65. <https://doi.org/10.1016/j.ymben.2015.02.005>.
- [10] Soong YV, Coleman SM, Liu N, Qin J, Lawton C, Alper HS, Xie D. Using oils and fats to replace sugars as feedstocks for biomanufacturing: challenges and opportunities for the yeast *Yarrowia lipolytica*. *Biotechnol Adv* 2023;65:108128. <https://doi.org/10.1016/j.biotechadv.2023.108128>.
- [11] Blazeck J, Hill A, Liu L, Knight R, Miller J, Pan A, Otoupal P, Alper HS. Harnessing *Yarrowia lipolytica* lipogenesis to create a platform for lipid and biofuel production. *Nat Commun* 2014;5:3131. <https://doi.org/10.1038/ncomms4131>.
- [12] Michely S, Gaillardin C, Nicaud JM, Neugeglise C. Comparative physiology of oleaginous species from the *Yarrowia* clade. *PLoS One* 2013;8(5):e63356. <https://doi.org/10.1371/journal.pone.0063356>.
- [13] Zhou K, Yu C, Liang N, Xiao W, Wang Y, Yao M, Yuan Y. Adaptive evolution and metabolic engineering boost lycopene production in *Saccharomyces cerevisiae* via enhanced precursors supply and utilization. *J Agric Food Chem* 2023;71:3821–31. <https://doi.org/10.1021/acs.jafc.2c08579>.
- [14] Darvishi F, Destain J, Nahvi I, Thonart P, Zarkesh-Esfahani H. High-level production of extracellular lipase by *Yarrowia lipolytica* mutants from methyl oleate. *N Biotech* 2011;28:756–60. <https://doi.org/10.1016/j.nbt.2011.02.002>.
- [15] Michely S, Gaillardin C, Nicaud JM, Neugeglise C. Comparative physiology of oleaginous species from the *Yarrowia* clade. *PLoS One* 2013;8:e63356. <https://doi.org/10.1371/journal.pone.0063356>.
- [16] Sassi H, Delvigne F, Kar T, Nicaud JM, Coq AM, Steels S, Fickers P. Deciphering how *LIP2* and *POX2* promoters can optimally regulate recombinant protein production in the yeast *Yarrowia lipolytica*. *Microb Cell Factories* 2016;15(1):159. <https://doi.org/10.1186/s12934-016-0558-8>.
- [17] Beopoulos A, Haddouche R, Kabran P, Dulerio T, Chardot T, Nicaud JM. Identification and characterization of DGA2, an acyltransferase of the DGAT1 acyl-CoA:diacylglycerol acyltransferase family in the oleaginous yeast *Yarrowia lipolytica*. New insights into the storage lipid metabolism of oleaginous yeasts. *Appl Microbiol Biotechnol* 2012;93:1523–37. <https://doi.org/10.1007/s00253-011-3506-x>.
- [18] Tai M, Stephanopoulos G. Engineering the push and pull of lipid biosynthesis in oleaginous yeast *Yarrowia lipolytica* for biofuel production. *Metab Eng* 2013;15:1–9. <https://doi.org/10.1016/j.ymben.2012.08.007>.
- [19] Zhang H, Damude HG, Yadav NS. Three diacylglycerol acyltransferases contribute to oil biosynthesis and normal growth in *Yarrowia lipolytica*. *Yeast* 2012;29(1):25–38. <https://doi.org/10.1002/yea.1914>.
- [20] Zhang Y, Wang Y, Yao M, Liu H, Zhou X, Xiao W, Yuan Y. Improved campesterol production in engineered *Yarrowia lipolytica* strains. *Biotechnol Lett* 2017;39:1033–9. <https://doi.org/10.1007/s10529-017-2331-4>.



- [21] Blazeck J, Liu L, Knight R, Alper HS. Heterologous production of pentane in the oleaginous yeast *Yarrowia lipolytica*. *J Biotechnol* 2013;165(3–4):184–94. <https://doi.org/10.1016/j.jbiotec.2013.04.003>.
- [22] Guo Q, Peng QQ, Chen YY, Song P, Ji XJ, Huang H, Shi TQ. High-yield  $\alpha$ -humulene production in *Yarrowia lipolytica* from waste cooking oil based on transcriptome analysis and metabolic engineering. *Microb Cell Factories* 2022;21:271. <https://doi.org/10.1186/s12934-022-01986-z>.
- [23] Xie D, Jackson EN, Zhu Q. Sustainable source of omega-3 eicosapentaenoic acid from metabolically engineered *Yarrowia lipolytica*: from fundamental research to commercial production. *Appl Microbiol Biotechnol* 2015;99:1599–610. <https://doi.org/10.1007/s00253-014-6318-y>.
- [24] Xie D, Miller E, Sharpe P, Jackson E, Zhu Q. Omega-3 production by fermentation of *Yarrowia lipolytica*: from fed-batch to continuous. *Biotechnol Bioeng* 2017;114:798–812. <https://doi.org/10.1002/bit.26216>.
- [25] Worland AM, Czajka JJ, Xing Y, Harper Jr WF, Moore A, Xiao Z, et al. Analysis of *Yarrowia lipolytica* growth, catabolism, and terpenoid biosynthesis during utilization of lipid-derived feedstock. *Metab Eng Commun* 2020;11:e00130. <https://doi.org/10.1016/j.mec.2020.e00130>.
- [26] Nasution O, Lee YM, Kim E, Lee Y, Kim W, Choi W. Overexpression of OLE1 enhances stress tolerance and constitutively activates the MAPK HOG pathway in *Saccharomyces cerevisiae*. *Biotechnol Bioeng* 2017;114(3):620–31. <https://doi.org/10.1002/bit.26093>.
- [27] Fang Z, Chen Z, Wang S, Shi P, Shen Y, Zhang Y, Xiao J, Huang Z. Overexpression of OLE1 enhances cytoplasmic membrane stability and confers resistance to cadmium in *Saccharomyces cerevisiae*. *Appl Environ Microbiol* 2017;83(1). <https://doi.org/10.1128/aem.02319-16>.
- [28] Larroude M, Celińska E, Back A, Thomas S, Nicaud J-M, Ledesma-Amaro R. A synthetic biology approach to transform *Yarrowia lipolytica* into a competitive biotechnological producer of  $\beta$ -carotene. *Biotechnol Bioeng* 2018;115:464–72.
- [29] Wei LJ, Cao X, Liu JJ, Kwak S, Jin YS, Wang W, Hua Q. Increased accumulation of squalene in engineered *Yarrowia lipolytica* through deletion of PEX10 and URE2. *Appl Environ Microbiol* 2021;87(17):e0048121. <https://doi.org/10.1128/AEM.00481-21>.
- [30] Marsafari M, Azi F, Dou S, Xu P. Modular co-culture engineering of *Yarrowia lipolytica* for amorphadiene biosynthesis. *Microb Cell Factories* 2022;21(1):279. <https://doi.org/10.1186/s12934-022-02010-0>.
- [31] Marsafari M, Azi F, Dou S, Xu P. Modular co-culture engineering of *Yarrowia lipolytica* for amorphadiene biosynthesis. *Microb Cell Factories* 2022;21:279. <https://doi.org/10.1186/s12934-022-02010-0>.
- [32] Wang L, Liu Z, Jiang H, Mao X. Biotechnology advances in  $\beta$ -carotene production by microorganisms. *Trends Food Sci Technol* 2021;111:322–32. <https://doi.org/10.1016/j.tifs.2021.02.077>.
- [33] Wang C, Zhao S, Shao X, Park JB, Jeong SH, Park HJ, Kwak WJ, Wei G, Kim SW. Challenges and tackles in metabolic engineering for microbial production of carotenoids. *Microb Cell Factories* 2019;18(1):55. <https://doi.org/10.1186/s12934-019-1105-1>.
- [34] Du HX, Xiao WH, Wang Y, Zhou X, Zhang Y, Liu D, Yuan YJ. Engineering *Yarrowia lipolytica* for campesterol overproduction. *PLoS One* 2016;11:e0146773. <https://doi.org/10.1371/journal.pone.0146773>.
- [35] Klumpp S, Scott M, Pedersen S, Hwa T. Molecular crowding limits translation and cell growth. *Proc Natl Acad Sci USA* 2013;110:16754–9. <https://doi.org/10.1073/pnas.1310377110>.
- [36] Liu Y, Su A, Tian R, Li J, Liu L, Du G. Developing rapid growing *Bacillus subtilis* for improved biochemical and recombinant protein production. *Metab Eng Commun* 2020;11:e00141. <https://doi.org/10.1016/j.mec.2020.e00141>.